American Mineralogist, Volume 87, pages 775–779, 2002

Experimental evidence of three coexisting immiscible fluids in synthetic granitic pegmatite

ILYA V. VEKSLER,* RAINER THOMAS, AND CHRISTIAN SCHMIDT

GeoForschungsZentrum Potsdam, Telegrafenberg D-14473, Potsdam, Germany

ABSTRACT

We present an experimental study of synthetic peraluminous granite doped with H_2O, B, P, and F, which confirms that aluminosilicate melt, hydrous fluid, and hydrosaline melt (high-temperature brine) can stably coexist at 450–900 °C and 0.1–0.2 GPa in bulk compositions similar to those of natural granitic pegmatites. Hydrosaline melt is not quenchable, unstable at room conditions, and requires special techniques for synthesis and preservation. Raman spectroscopy and electron microprobe analyses of hydrosaline melt synthesized in our experiments show that it is composed of H_3BO_3, Na_3AlF_6, $AlPO_4$, H_2O, and aluminosilicate components. Aluminosilicate melt saturated in both hydrosaline liquid and hydrous fluid at 850 °C and 0.2 GPa contains 3.6 wt% F, 4.2 wt% P_2O_5, and 4 wt% B_2O_3. Natural hydrosaline melts have previously been found as inclusions trapped in rock-forming minerals. They are not restricted to granites and can be effective agents for enhanced crystal growth, metasomatism, and ore formation. In addition, hydrosaline melts may account for many characteristic features of rare-element and miarolitic pegmatites, such as giant size and perfect shapes of crystals in pegmatite cores, diverse mineralogy, and strong enrichment in rare elements.

INTRODUCTION

Granitic pegmatites, especially rare-element varieties, attract much attention as a source of gemstones and rare-metal ores (e.g., Ta, Be, and Cs). Such pegmatites are among the most compositionally complex igneous rocks and show extreme enrichment in a broad range of elements including volatiles and fluxes. Classical theories of pegmatite formation (e.g., Jahns and Burnham 1969) emphasize the importance of volatiles (primarily H_2O) and state that granitic pegmatites crystallize from coexisting aluminosilicate melt and hydrous fluid. Other models downplay the role of a separate fluid phase and suggest that aluminosilicate melts can produce highly evolved pegmatitic liquids via continuous crystallization under particular kinetic conditions (London 1986, 1992, 1999).

The topology of salt-water systems, such as NaCl-H_2O (Sourirajan and Kennedy 1962), shows that over a wide range of *P-T-X* conditions, fluid separates into a low-salinity vapor and a high-salinity liquid (brine). If such a two-phase field extends to temperatures exceeding the silicate solidus, and if the vapor and the brine do not dissolve completely in silicate melt, a three-fluid equilibrium (melt + brine + vapor) is reached (Bodnar et al. 1985; Shmulovich and Churakov 1998). The expected range of *P* and *T* for the three-phase equilibrium is well within that of natural pegmatite magmas (0.1–0.3 GPa, 500–700 °C) and the coexistence of three fluids is most likely for shallow-level, B-, F-, and P-rich pegmatites. Natural occurrences of three contrasting types of melts and fluids have been observed as inclusions in quartz and other minerals from granitic pegmatites worldwide (Roedder 1992). These observations led to a suggestion that late stages of magma evolution in the pegmatite system involve three immiscible fluids: aluminosilicate melt, hydrous fluid, and hydrosaline melt (or concentrated brine). However, experiments in related synthetic systems have never shown more than two fluids (London 1992), and it has been argued that the three types of inclusions represent consecutive, rather than coexisting fluids. Here we present the first conclusive evidence of the three-phase fluid equilibrium in a synthetic silicic system similar in bulk composition to the most flux-rich pegmatite magmas. In our experiments, three-fluid immiscibility is achieved at concentrations of B, P, and F in aluminosilicate melt similar to those reached in natural pegmatitic melts. Our results support the inference of immiscibility from inclusion studies, and encourage rethinking some of the classical concepts of pegmatite genesis as well as the nature of magmatic fluid-melt equilibria in general.

EXPERIMENTAL METHODS AND RESULTS

Starting composition

A starting glass with the bulk composition (in wt%): SiO_2 = 58.7, Al_2O_3 = 16.5, B_2O_3 = 5.0, Na_2O = 2.9, K_2O = 3.7 Rb_2O = 1.1, Cs_2O = 1.0, Li_2O = 0.5, P_2O_5 = 4.2, F 4.6, and H_2O = 1.5 was synthesized from reagent-grade chemicals in cold-seal pressure vessel at 900 °C and 2 GPa. The glass is strongly peraluminous, with the molar Al_2O_3 / (Li_2O + Na_2O + K_2O + Rb_2O + Cs_2O) = 1.46, and models the most-enriched compositions of melt inclusions found in pegmatite quartz (Thomas et al. 2000).

* E-mail: veksler@gfz-potsdam.de

Analytical methods

Major elements in run products (except B and Li) were analyzed with a Cameca SX-100 electron microprobe in WDS mode at 10 nA beam current and accelerating voltage of 15 kV. Glasses were analyzed with a broad beam (beam size of 20–40 μm). Boron was analyzed with a Cameca SX-50 microprobe, equipped with the PC2 pseudo-crystal for light elements, at counting time of 300 s, 10 kV, and 40 nA using an anti-contamination cold trap cooled by liquid nitrogen. Confocal Raman spectroscopy was carried out using a Dilor XY Laser Raman Triple 800 mm spectrometer and an Olympus optical microscope (see Thomas 2001, 2002 for the details).

In situ studies in hydrothermal diamond cell

The first crucial evidence for 3-fluid equilibrium was obtained from observations in a hydrothermal diamond-anvil cell (HDAC, Bassett et al. 1993), which allows direct visual observation of phase transitions and in situ Raman spectroscopy at elevated P and T. Anvils of our cell were 0.9 mm in diameter and made of ultra-low fluorescence, type Ia diamond. We used a Re gasket with uncompressed thickness of 125 μm and a sample chamber of 0.4 mm in diameter. In the HDAC experiments, homogeneous synthetic glass and spectroscopic grade water were loaded into the sample chamber. Some water was allowed to leak out of the chamber before sealing so that it contained a vapor bubble. Because the volume of the sample chamber remained essentially constant during heating runs, the pressure was estimated from the temperature at which the vapor bubble disappeared using the equation of state of pure water. The effect of dissolved components such as H_3BO_3 on water isochores was ignored due to the lack of appropriate data.

The first visible changes during heating were disappearance of the vapor bubble at 310–350 °C and devitrification and melting of the glass (starting respectively at about 350 and 500 °C). Visual observations and Raman spectra (see below) suggested that the glass transition temperature, T_g, was reached at about 350–400 °C. Movement of the melt droplet at temperatures above 450 °C indicated that the viscosity of the melt was low. Further heating caused melting of crystals immersed in the melt and mutual dissolution and equilibration of melt and fluid. From 800 °C to the maximum P-T conditions reached in our runs (840 °C and roughly 0.4 GPa), the sample appeared to represent simple two-phase silicate melt-hydrous fluid equilibrium.

Hydrosaline melt became apparent during subsequent cooling when droplets nucleated and grew inside aluminosilicate liquid as illustrated in Figure 1. We believe that the hydrosaline phase was present earlier during the heating because, as described below, it tends to form thin films on surfaces and can be almost invisible. During further cooling, mutual solubility of the three fluid phases noticeably decreased and the globules grew in size. Crystallization started around 800 °C and proceeded in the presence of three fluid phases until the aluminosilicate solidus was reached at about 450 °C. The described sequence of phase transitions was reproduced with the same charge in repeated heating-cooling cycles and, therefore, we believe that significant deviations from equilibrium are unlikely.

Raman spectra obtained during HDAC experiments focused on the distribution and speciation of B. This element is moderately incompatible with the structure of aluminosilicate melts and has a strong affinity to hydrous fluids. The high concentrations of B in our charges are likely to be among the main driving forces for fluid unmixing and the formation of hydrosaline liquid. Of the three fluid phases, only aluminosilicate melt and hydrous fluid were large enough to obtain unambiguous single-phase spectra. The intensities of B bands suggest high B concentrations in both phases. All B in the fluid phase was in trigonal planar $B(OH)_3$ groups, while speciation in the melt was more complex (see Fig. 2 for more details).

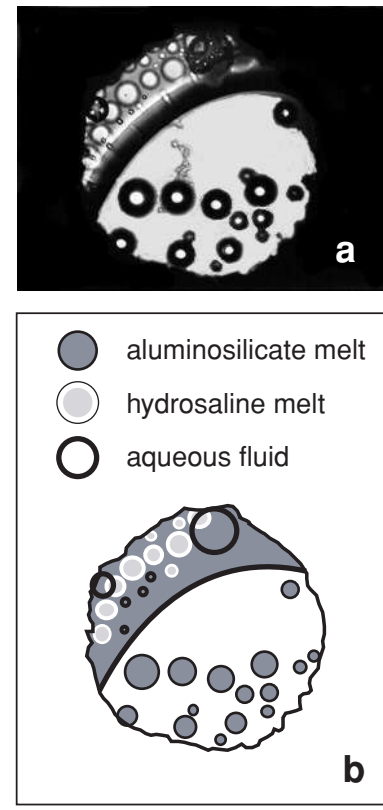

FIGURE 1. Photomicrograph (**a**) and explanatory sketch (**b**) of a plan view into the sample chamber of HDAC during slow cooling from 830 to 810 °C and ~0.4 GPa. Globules of hydrosaline melt and fluid bubbles nucleated and grew inside aluminosilicate melt while beads of the aluminosilicate melt precipitated from the hydrous fluid implying close approach to thermodynamic equilibrium. The diameter of the sample chamber is 0.4 mm.

Dynamic and static runs in cold-seal pressure vessels

To obtain larger samples for chemical study required synthesis in rapid-quench, cold-seal pressure vessels. The main experimental difficulty here is that neither the hydrosaline melt nor hydrous fluid are quenchable, even at cooling rates of hundreds of degrees per second. However, we discovered that these phases can be preserved in run products if they form globules or bubbles enclosed in aluminosilicate glass. This condition was achieved by means of short-duration, dynamic runs similar in principle to the isochoric HDAC experiments.

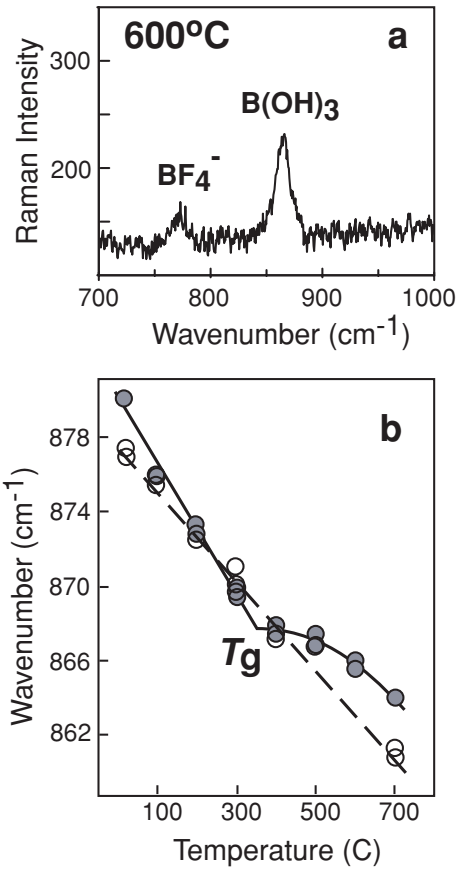

FIGURE 2. Speciation of B according to in situ Raman studies in the HDAC. (**a**) A typical Raman spectrum of the melt at 600 °C showing bands assigned to $B(OH)_3$ and BF_4^{1-} species. The latter band is absent in the fluid phase and very weak in aluminosilicate glass below the glass transition temperature (T_g). (**b**) With rising T, the band assigned to $B(OH)_3$ shifts to higher frequencies. The shift is almost linear in the fluid (open circles and dashed line), but in the melt (gray circles and solid curve) it shows an inflection at T_g.

Figure 3 shows an example of hydrosaline globules synthesized in this way. The globules were too unstable for electron microprobe analysis, but key chemical features were revealed using Raman spectroscopy. Raman spectra of the globules and the host glass showed a broad asymmetric band in the 490 cm^{-1} region, assigned to oxygen vibrations in the aluminosilicate network, bands assigned to $B(OH)_3$ (at about 500 and 880 cm^{-1}), and $AlPO_4$ complexes (at 1100 cm^{-1}, Mysen 1998). In addition, the hydrosaline globules revealed traces of tetrafluoroborate BF_4^{1-} (a band at about 776 cm^{-1}, Lutz et al. 1996) and BPO_4 units (weak bands at 540 and 635 cm^{-1}, Adamczyk and Handke 2000). The intensity of the main $B(OH)_3$ band at 880 cm^{-1} was much higher in the globules than in the host glass, and from these intensities B_2O_3 concentrations were estimated (Thomas 2002) to be 6.8 wt% in the globules and 3.1 wt% in the surrounding glass. In the high-frequency region, the difference in the shape and intensity of the broad 3000–4000 cm^{-1} band is very similar to that observed previously in two different types

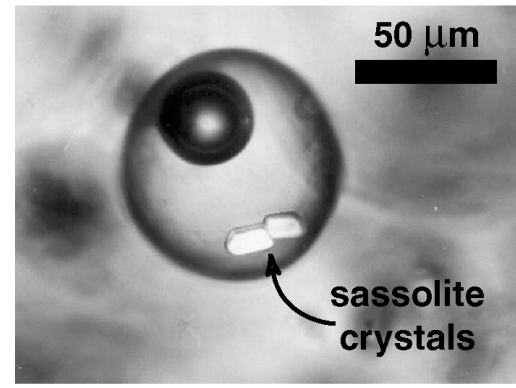

FIGURE 3. A globule of hydrosaline immiscible melt in aluminosilicate glass. The globules were synthesized in rapid-quench cold-seal pressure vessels by isochoric cooling from 900 °C and 0.2 GPa at 10 °C/min. Hydrosaline melt quenches to amorphous gel containing a shrinkage bubble with double meniscus. The gel-like amorphous material in the globules is very unstable and starts to exsolve daughter sassolite (H_3BO_3) crystals within a few hours after the quench.

of natural melt inclusions hosted in pegmatite quartz (Thomas et al. 2000). Estimations of bulk H_2O content based on the 3000–4000 cm^{-1} band intensity (Thomas 2000) are 11 wt% in the host glass and up to 43 wt% in the hydrosaline globules. Although speciation in the quenched globules at room temperature may not fully represent species in the original hydrosaline melt at elevated P and T, the abundant $B(OH)_3$ and BF_4^{1-} and other details correspond well with the in situ spectra obtained in HDAC experiments.

Finally, using conventional long-duration static runs at lower temperatures, we obtained pools of quenched hydrosaline melt large and solid enough for electron microprobe analyses (Fig. 4). Hydrosaline melt was preserved as surface films on precipitating crystals and interstitial fillings in glass-crystal aggregates. Determination of its bulk composition is hampered by the extreme heterogeneity of such pools due to secondary, quench segregation of hydrosaline melt into at least two different glasses and a number of crystalline solids. Therefore, one should treat the analyses of hydrosaline pools and globules as approximate estimations. According to the average of broad-beam (30–40 μm) analyses, the solid part of hydrosaline melt contains (in wt%): SiO_2 = 23.2, Al_2O_3 = 21.4, B_2O_3 = 15.6, Na_2O = 5.1, K_2O = 2.4, Rb_2O = 1.1, Cs_2O = 1.0, P_2O_5 = 2.6, F = 17.5, the remaining 18% being mostly H_2O and minor Li_2O. These results demonstrate that the hydrosaline melt is strongly enriched in F and B (more than 3 times that of the aluminosilicate glass) and effectively fractionates Na from K (the molar Na/K = 3.2 in the hydrosaline melt vs. 1.4 in the aluminosilicate glass). Decoupling of alkalis is likely to result from different affinities of Na and K to alumionfluoride species (Gramenitskiy and Shchekina 1994).

DISCUSSION

One of the key open questions concerning the genesis of granitic pegmatites is whether they are formed from a single homogenous parental liquid (London 1999), or from a mixture of genetically related fluid phases (Roedder 1992; Jahns and

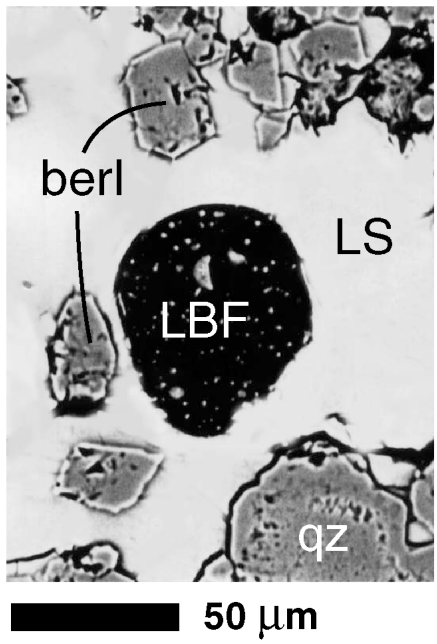

FIGURE 4. Backscattered electron image of products of a long-duration (100 hours) run at 550 °C and 0.2 GPa showing a pool of the B- and F-rich hydrosaline melt (LBF) in aluminosilicate glass (LS). Crystal phases are berlinite (berl) and quartz (qz). Hydrosaline melt quenches to heterogeneous mixture of crystal phases, glass and possibly also some aqueous solution.

Burnham 1969). Our study strongly suggests that there may be in fact as many as three coexisting fluids involved in pegmatite formation, but the chemical and thermodynamic limits on the three-fluid equilibrium still have to be established. Recently, Sowerby and Keppler (2002) observed complete miscibility between aluminosilicate melt and hydrous fluid at 0.5 GPa and 595 °C in HDAC experiments with B- and F-rich peralkaline synthetic pegmatite. Thus, the position of the critical curve in *P-T* space appears to be strongly affected by bulk chemistry of the system and especially by the ratio of alumina to alkalis.

Implications of the hydrosaline melt for pegmatites are profound. The observed wetting properties of hydrosaline melt make it very mobile in magmatic systems at the final stages of crystallization, and this property may explain why hydrosaline inclusions are so abundant in pegmatite minerals. This melt is an effective flux for crystal growth and may account for many characteristic features of miarolitic and rare-element pegmatites, such as giant size and perfect shapes of crystals in pegmatite cores, diverse mineralogy, and strong local enrichment in rare elements.

Spectacular local variations in the sizes and proportion of main rock-forming minerals and extensive chemical zoning are typical for pegmatites. Many of these features, especially at a scale of individual crystals, may result from disequilibrium crystallization and boundary layer effects (London 1992, 1999). But at a scale relevant to whole pegmatitic bodies, fluid immiscibility and gravitational phase separation, enhanced by wetting properties and the low viscosity of flux-rich pegmatitic fluids, should provide much more effective means of chemical differentiation. For example, London (1992) pointed out that curved shapes of aplite bodies and their sharp contacts with massive quartz in Tanco pegmatite (Manitoba), resembled interfaces between two immiscible fluids. In light of new experimental evidence presented here, this resemblance may indeed reflect the percolation of aluminosilicate and hydrosaline melts, both of which should contain, at such a late stage of pegmatite evolution, significant proportions of crystals.

Three-fluid equilibria in high-temperature inorganic systems are not uncommon and natural occurrences are not restricted to granitic pegmatites. Formation of chloride hydrosailne melts has been demonstrated experimentally (Koster van Groos and Wyllie 1969; Shinohara et al. 1989) and simultaneous exsolution of the brine and dilute aqueous vapor is likely to be common in rhyolites and shallow-level granitic intrusions (Shinohara 1994). The presence of Cl is likely to increase miscibility gaps between the three fluids. Immiscible silicate and carbonate melts accompanied by CO_2 vapor provide another geologically relevant example of three-fluid immiscibility (Koster van Groos and Wyllie 1966) and high-salinity inclusions are very common in carbonatites, especially in apatite (e.g., Andersen 1986). Recent studies of fluid inclusions have led to a growing recognition of the importance of high-temperature brine-vapor phase separation for magmatic ore deposits, such as skarns, Cu-porphyry, and Sn-W ores (Heinrich et al. 1999; Fulignati et al. 2001; Kamenetsky et al. 1999). Because hydrosaline melts are hard to detect in run products, we suggest that many classical silicate-salt-H_2O systems should be re-examined. Also, the possibility of a second immiscible and unquenchable fluid phase should be kept in mind during experimental studies of fluid-melt element partitioning. The importance of hydrosaline melts in nature may extend far beyond the cases of extremely evolved igneous rocks examined here to large-scale melt-fluid interactions, e.g., mantle metasomatism and melting in subduction zones.

ACKNOWLEDGMENTS

We thank Drs. Wilhelm Heinrich and Robert Trumbull for fruitful discussions and help in preparation of this paper. Detailed and constructive reviews by Drs. Robert Dymek, John Sowerby, and James Webster helped to improve the original manuscript. This study was supported by the grant of DFG priority program "Formation, transport and differentiation of silicate melts" ("Bildung, Transport und Differenzierung von Silikatschmelzen") SPP TH 489/2-1.

REFERENCES CITED

Adamczyk, A. and Handke, M. (2000) The isotopic effect and spectroscopic studies of boron orthophosphate (BPO_4). Journal of Molecular Structure, 555, 159–164.

Andersen, T. (1986) Magmatic fluids in the Fen carbonatite complex, S. E. Norway. Evidence of mid-crustal fractionation from solid and fluid inclusions in apatite. Contributions to Mineralogy and Petrology, 93, 491–503.

Bassett, W.A., Shen, A.H., Bucknum, M., and Chou, I-M. (1993) A new diamond anvil cell for hydrothermal studies to 2.5 GPa and from –190 to 1200 °C. Review of Scientific Instruments, 64, 2340–2345.

Bodnar, R.J., Burnham, C.W., and Sterner, S.M. (1985) Synthetic fluid inclusions in natural quartz. III. Determination of phase equilibrium properties in the system H_2O-NaCl to 1000°C and 1500 bars. Geochimica et Cosmochimica Acta, 49, 1861–1873.

Fulignati, P., Kamenetsky, V.S., Marianelli, P., Sbrana, A., and Mernagh, T.P. (2001) Melt inclusion record of immiscibility between silicate, hydrosaline, and carbonate melts: Applications to skarn genesis at Mount Vesuvius. Geology, 29, 1043–1046.

Gramenitskiy, Ye., N., and Shchekina, T.I. (1994) Phase relationships in the liquidus part of a granitic system containing flourine. Geochemistry International, 31, 52–70.

Heinrich, C.A., Günther, D., Audétat, A., Ulrich, T., and Frischknecht, R. (1999) Metal fractionation between magmatic brine and vapor, determined by mi-

croanalysis of fluid inclusions. Geology, 27, 755–758.
Jahns, R.H. and Burnham, C.W. (1969) Experimental studies of pegmatite genesis: I. A model for the derivation and crystallization of granitic pegmatites. Economic Geology, 64, 843–864.
Kamenetsky, V.S., Wolfe, R.C., Eggins, S.M., Mernagh, T.P., and Bastrakov, E. (1999) Volatile exsolution at the Dinkidi Cu-Au porphyry deposit, Philippines: A melt inclusion record of the initial ore-forming process. Geology, 27, 691–694.
Koster van Groos, A.F. and Wyllie, P.J. (1966) Liquid immiscibility in the system Na_2O-Al_2O_3-SiO_2-CO_2 at pressures up to 1 kilobar. American Journal of Science, 264, 234–255.
———(1969) Melting relationships in the system $NaAlSi_3O_8$-NaCl-H_2O at one kilobar pressure, with petrological applications. Journal of Geology, 77, 581–605.
London, D.(1986) Magmatic-hydrothermal transition in the Tanco rare-element pegmatite: Evidence from fluid inclusions and phase equilibrium experiments. American Mineralogist, 71, 376–395.
———(1992) The application of experimental petrology to the genesis and crystallization of granitic pegmatites. Canadian Mineralogist, 30, 499–540.
———(1999) Melt boundary layers and the growth of pegmatite textures. Canadian Mineralogist, 37, 826–827.
Lutz, H.D., Himmrich, J., and Schmidt, M. (1996) Lattice vibration spectra. Part LXXXVI. Infrared and Raman spectra of baryte-type $TlClO_4$, $TlBF_4$, and NH_4BF_4 single crystals and of ^{11}B-enriched NH_4BF_4. Journal of Alloys and Compounds, 241, 1–9.
Mysen, B.O. (1998) Phosphorus solubility mechanisms in haplogranitic aluminosilicate glass and melt: effects of temperature and aluminium content. Contributions to Mineralogy and Petrology, 133, 38–50.
Roedder, E. (1992) Fluid inclusion evidence for immiscibility in magmatic differentiation. Geochimica et Cosmochimica Acta, 56, 5–20.
Shinohara, H. (1994) Exsolution of immiscible vapor and fluid phases from a crystallizing silicate melt: Implications for chlorine and metal transport. Geochimica et Cosmochimica Acta, 58, 4215–5221.
Shinohara, H., Ilyama, J.T., and Matsuo, S. (1989) Partition of chlorine compounds between silicate melt and hydrothermal solutions: I. Partition of NaCl-KCl. Geochimica et Cosmochimica Acta, 53, 2617–2630.
Shmulovich, K.I. and Churakov, S.V. (1998) Natural fluid phases at high temperatures and low pressures. Journal of Geochemical Exploration, 62, 183–191.
Sourirajan, S. and Kennedy, G.C. (1962) The system H_2O-NaCl at elevated temperatures and pressures. American Journal of Science, 260, 115–141.
Sowerby, J. and Keppler, H. (2002) The effect of fluorine, boron and excess sodium on the critical curve in the albite–H_2O system. Contributions to Mineralogy and Petrology, in press.
Thomas, R. (2000) Determination of water contents of granite melt inclusions by confocal laser Raman microprobe spectroscopy. American Mineralogist, 85, 868–872.
———(2002) Determination of the H_3BO_3 concentration in melt and fluid inclusions in granite pegmatites by laser Raman spectroscopy. American Mineralogist, 87, 56–68.
Thomas, R., Webster, J.D., and Heinrich, W. (2000) Melt inclusions in pegmatite quartz: complete miscibility between silicate melts and hydrous fluids at low pressure. Contributions to Mineralogy and Petrology, 139, 394–401.

MANUSCRIPT RECEIVED DECEMBER 6, 2001
MANUSCRIPT ACCEPTED FEBRUARY 3, 2002
MANUSCRIPT HANDLED BY ROBERT F. DYMEK